



Research paper

SLC1A1 mediated glutamine addiction and contributed to natural killer T-cell lymphoma progression with immunotherapeutic potential



Jie Xiong^{a,1}, Nan Wang^{a,1}, Hui-Juan Zhong^{a,1}, Bo-Wen Cui^{a,1}, Shu Cheng^a, Rui Sun^a, Jia-Yi Chen^b, Peng-Peng Xu^a, Gang Cai^b, Li Wang^{a,c}, Xiao-Jian Sun^a, Jin-Yan Huang^a, Wei-Li Zhao^{a,c,*}

^a Shanghai Institute of Hematology, State Key Laboratory of Medical Genomics, National Research Center for Translational Medicine, Ruijin Hospital affiliated to Shanghai Jiao Tong University School of Medicine, Shanghai, China

^b Department of Radiation, Shanghai Rui Jin Hospital, Shanghai Jiao Tong University School of Medicine, Shanghai, China

^c Pôle de Recherches Sino-Français en Science du Vivant et Génomique, Laboratory of Molecular Pathology, Shanghai, China

ARTICLE INFO

Article History:

Received 16 April 2021

Revised 22 September 2021

Accepted 22 September 2021

Available online xxx

Keywords:

Natural-killer T-cell lymphoma

Solute carrier family 1 member 1

EAAT3

Metabolomics

RNA-sequencing

Glutamine

Anti-PD-1 antibody

ABSTRACT

Background: Metabolic reprogramming plays an essential role on lymphoma progression. Dysregulation of glutamine metabolism is implicated in natural-killer T-cell lymphoma (NKTCL) and tumor cell response to asparaginase-based anti-metabolic treatment.

Methods: To understand the metabolomic alterations and determine the potential therapeutic target of asparaginase, we assessed metabolomic profile using liquid chromatography-mass spectrometry in serum samples of 36 NKTCL patients, and integrated targeted metabolic analysis and RNA sequencing in tumor samples of 102 NKTCL patients. The biological function of solute carrier family 1 member 1 (*SLC1A1*) on metabolic flux, lymphoma cell growth, and drug sensitivity was further examined in vitro in NK-lymphoma cell line NK-92 and SNK-6, and in vivo in zebrafish xenograft models.

Findings: In NKTCL patients, serum metabolomic profile was characterized by aberrant glutamine metabolism and *SLC1A1* was identified as a central regulator of altered glutaminolysis. Both in vitro and in vivo, ectopic expression of *SLC1A1* increased cellular glutamine uptake, enhanced glutathione metabolic flux, and induced glutamine addiction, leading to acceleration of cell proliferation and tumor growth. Of note, *SLC1A1* overexpression was significantly associated with *PD-L1* downregulation and reduced cytotoxic CD3+/CD8+ T cell activity when co-cultured with peripheral blood mononuclear cells. Asparaginase treatment counteracted *SLC1A1*-mediated glutamine addiction, restored *SLC1A1*-induced impaired T-cell immunity. Clinically, high EAAT3 (*SLC1A1*-encoded protein) expression independently predicted superior progression-free and overall survival in 90 NKTCL patients treated with asparaginase-based regimens.

Interpretation: *SLC1A1* functioned as an extracellular glutamine transporter, promoted tumor growth through reprogramming glutamine metabolism of NKTCL, while rendered tumor cells sensitive to asparaginase treatment. Moreover, *SLC1A1*-mediated modulation of *PD-L1* expression might provide clinical rationale of co-targeting metabolic vulnerability and immunosuppressive microenvironment in NKTCL.

Funding: This study was supported, in part, by research funding from the National Natural Science Foundation of China (82130004, 81830007 and 81900192), Chang Jiang Scholars Program, Shanghai Municipal Education Commission Gaofeng Clinical Medicine Grant Support (20152206 and 20152208), Clinical Research Plan of SHDC (2020CR1032B), Multicenter Clinical Research Project by Shanghai Jiao Tong University School of Medicine (DLY201601), Shanghai Chenguang Program (19CG15), Shanghai Sailing Program (19YF1430800), Medical-Engineering Cross Foundation of Shanghai Jiao Tong University (ZH2018QNA46), and Shanghai Yi Yuan Xin Xing Program.

© 2021 The Author(s). Published by Elsevier B.V. This is an open access article under the CC BY-NC-ND license (<http://creativecommons.org/licenses/by-nc-nd/4.0/>)

* Corresponding author at: Shanghai Institute of Hematology, State Key Laboratory of Medical Genomics, National Research Center for Translational Medicine, Ruijin Hospital affiliated to Shanghai Jiao Tong University School of Medicine, 197 Rui Jin Er Road, Shanghai 200025, China.

E-mail address: zhao.weili@yahoo.com (W.-L. Zhao).

¹ These authors equally contributed to this work.

1. Introduction

Natural killer T-cell lymphoma (NKTCL) is the most aggressive extranodal lymphoma and closely related to Epstein-Barr virus infection [1]. Recurrent somatic gene mutations are major genetic

Research in context

Evidence before this study

NKTCL is a malignant proliferation of CD56+/cytoCD3+ lymphocytes with aggressive clinical course and strong association of Epstein-Barr virus infection. Asparaginase-containing chemotherapy may target tumor cell metabolism and is effective in treating NKTCL. With clinical application of immune checkpoint inhibitors, it is imperative to understand the underlying mechanism of metabolic reprogramming with immune modulation in NKTCL.

Added value of this study

We assessed metabolomic profile using LC-MS and identified *SLC1A1* as a central regulator of aberrant glutamine metabolism in NKTCL. *SLC1A1* enhanced tumor cell proliferation in a glutamine-dependent manner, and independently predicted favorable clinical response to asparaginase-based regimens. More importantly, we found that *SLC1A1* downregulated PD-L1 expression and exhibited immunosuppressive activity. Asparaginase not only counteracted *SLC1A1*-mediated glutamine addiction, but also restored *SLC1A1*-induced impaired T-cell immunity.

Implications of all the available evidence

SLC1A1 induced aberrant glutamine metabolism and resulted in favorable prognosis to asparaginase-based anti-metabolic treatment in NKTCL. Co-targeting metabolic vulnerability and immunosuppressive microenvironment could be potential therapeutic strategy of NKTCL.

increased expression of *SLC2A5* enhances fructose utilization, exacerbates malignant phenotype and predicts inferior prognosis in acute myeloid leukemia [14] and in B-cell acute lymphoblastic leukemia [15]. *SLC7A5* is overexpressed in PTEN-/- T-cell acute lymphoblastic leukemia and related to leukemic transformation induced by PTEN deletion [16]. Solute carrier family 1 member 1 (*SLC1A1*, also known as EAAT3 for protein form), the predominant amino acid transporter of glutamate and aspartate [12], is associated with disease development and clinical outcomes in solid tumors such as breast cancer [17] and osteosarcoma [18]. In the present study, metabolomic profile of NKTCL was assessed and compared with that of DLBCL and PTCL, revealing aberrant glutamine metabolism in NKTCL. *SLC1A1* was overexpressed in NKTCL and mediated glutamine addiction, contributing to unique metabolomic feature with therapeutic potential.

2. Methods

2.1. Ethics statement

The study was approved by the Shanghai Ruijin Hospital review board and informed consent was obtained in accordance with the Declaration of Helsinki. The research program and all the related procedures were carried out according to standard operating procedures for Good Clinical Laboratory Practice standards (Ref no.: 2020-108).

2.2. Patients

Between July 2003 and May 2019, a total of 175 patients with newly diagnosed NKTCL, 34 patients with newly diagnosed PTCL, and 33 patients with newly diagnosed DLBCL, were included in this study (Figure S1). Histologic diagnoses were established according to WHO classification [19]. Serum samples (n=138) and tumor biopsies (n=175) of NKTCL patients were collected at diagnosis and further subjected to metabolomic assay (n=36), targeted metabolomic analysis (n=102), RNA-sequencing (RNA-seq, n=128), and immunohistochemistry (n=147). As for NKTCL treatment, induction regimens consisted of 4 to 8 cycles of CHOP/CHOP-like regimens (N=68) or 4 to 6 cycles of asparaginase-based regimens (MESA [methotrexate, etoposide, dexamethasone, and pegaspargase]/ESA [etoposide, dexamethasone, and pegaspargase] sandwiched with radiotherapy in 89 Ann Arbor stage I-II patients enrolled in NCT02825147 [6] and NCT02631239, and MESA in 18 Ann Arbor stage III-IV patients). Sixty-four age- and sex-matched healthy volunteers were referred as the control groups for metabolomics assay.

Baseline information was collected prospectively including patients' age, gender, ECOG performance status, Ann Arbor stage, Extranodal involvement, serum lactate dehydrogenase. The therapeutic regimens, treatment response and follow-up data was also prospectively collected (Table 1).

2.3. Metabolomic assay

Serum metabolomic profiles were assessed by liquid chromatography-mass spectrometry (LC-MS, Ultimate 3000LC, Orbitrap Elite Thermo, San Jose, CA, USA), as previously described [6]. Metabolic data were analyzed by SIEVE (Thermo) and SIMCA-P software (Umetrics AB, Umeå, Sweden). Quantification of targeted amino acids in serum samples and cells were assessed by high-performance liquid chromatography-mass spectrometry (LC-MS/MS, Shimadzu LC20AD, Kyoto, Japan and API 3200MD TRAP, Framingham, MA, USA) after pretreatment according to standard procedures [6].

2.4. RNA sequencing

Library construction was performed with Illumina TruSeq RNA Sample Prep Kit (Cat# RS-122-2001, RS-122-2002, for high quality

alterations of NKTCL, involving RNA helicase genes, tumor suppressors, JAK-STAT pathway, epigenetic modifiers, and RAS-MAPK pathway [2–4]. Integrating analysis of genomic and transcriptomic features of NKTCL, molecular subtypes have been revealed as the TSIM subtype (based on mutations in JAK-STAT pathway and *TP53*, as well as amp9p24.1/*JAK2* locus, amp17q21.2/*STAT3/5B/5A* locus, amp9p24.1/*PD-L1/2* locus, and del6q21), the MB subtype (based on *MGA* mutation and 1p22.1/*BRDT* LOH), and the HEA subtype (based on *HDAC9*, *EP300*, and *ARID1A* mutation), which differ in cell of origin, Epstein-Barr virus gene expression, transcriptional signatures, and therapeutic targets [5]. Metabolic reprogramming is another hallmark of lymphoma progression and has also provided clues for NKTCL therapy [6]. Primarily resistant to anthracycline-based chemotherapy, clinical outcomes of the NKTCL patients are significantly improved by asparaginase-based anti-metabolic treatment [7]. Aberrant glutamine metabolism attributes to asparagine synthesis of NKTCL cells and response to asparaginase [6]. Previous report showed that asparagine synthetase (*ASNS*) gene encodes the enzyme catalyzed the synthesis of asparagine from aspartate and glutamine, and indicates asparaginase resistance in NKTCL [8]. It is therefore important to better understand the metabolomic feature and determine the potential therapeutic target of asparaginase in NKTCL.

Tumor-derived metabolites detected in serum represent major cancer by-products [9]. As our previous reports in peripheral T-cell lymphoma (PTCL) and diffuse large B-cell lymphoma (DLBCL), distinct serum metabolomics offer reliable biomarkers of diagnosis, prognosis prediction and disease monitoring [10,11]. Solute carrier (SLC) family is one of the main transporter superfamilies, transporting inorganic ions, sugars, and amino acids needed for cell growth and vital cellular processes [12]. In cancer cells, dysregulation of SLC family leads to metabolic reprogramming and tumor progression [13]. For example,

Table 1
Comparison of clinical characteristics of NKTL patients according to tumor EAAT3 expression (n=147).

	High EAAT3 expression (n=117)	Low EAAT3 expression (n=30)	P value
Age			
≤60 years	93 (79.5%)	23 (76.7%)	0.735
>60 years	24 (20.5%)	7 (23.3%)	
Gender			
Female	39 (33.3%)	9 (30.0%)	0.728
Male	78 (66.7%)	21 (70.0%)	
ECOG performance status			
0/1	94 (80.3%)	24 (80.0%)	0.967
≥2	23 (19.7%)	6 (20.0%)	
Ann Arbor stage			
I-II	99 (84.6%)	22 (73.3%)	0.149
III-IV	18 (15.4%)	8 (26.7%)	
Extranodal involvement			
0/1	100 (85.5%)	24 (80.0%)	0.462
≥2	17 (14.5%)	6 (20.0%)	
Serum lactate dehydrogenase			
Normal	59 (50.4%)	16 (53.3%)	0.776
Increased	58 (49.6%)	14 (46.7%)	
Regimens			
Asparaginase-based	71 (60.7%)	19 (63.3%)	0.790
Anthracycline-based	46 (39.3%)	11 (36.7%)	
Treatment response*			
Overall response rate (ORR)	63 (88.7%)	10 (52.6%)	<0.001
Complete remission rate (CR)	61 (85.9%)	10 (52.6%)	0.002

P values were calculated by Pearson's chi-square test.

* Treatment response was analyzed in patients receiving asparaginase-based regimens.

frozen samples, n=84) and TruSeq RNA Exome Prep Kit (Cat# 20020189, 20020490, and 20020183, for low quality frozen samples and FFPE samples, n=44). Paired-end sequencing was performed using Illumina HiSeq X10. The raw RNA-seq reads were aligned to human reference genome hg19 using Hisat2 (v2.0.5) [20] and STAR (v2.5.2b) [21]. All gene expression levels in RNA-seq data were estimated as previously described [5].

2.5. Immunohistochemistry

Immunohistochemistry was performed with commercial antibodies anti-EAAT3 antibody (Cat# ab124802, RRID: 10974334, Abcam, Cambridge, UK) or anti-ASNS antibody (Cat# ab126254, RRID: 11127885, Abcam). Protein expression was scored semi-quantitatively based on staining intensity (SI) and percentage of positive cells (PP) [22]. Immunoreactive score=SI×PP. SI was determined as 0, negative; 1, weak; 2, moderate; and 3, strong. PP was defined as 1, <25%; 2, 25-50%; 3, 50-75%; and 4, 75-100% positive cells. Immunoreactive score <4 was referred as “- /+” (Low EAAT3 or ASNS expression), Immunoreactive score ≥4 was “+++” (High EAAT3 or ASNS expression).

2.6. Cell line and reagents

Natural-killer cell line NK-92 (Cat# CRL-2407) was available from American Type Culture Collection (Manassas, VA, USA). SNK-6 was kindly provided by Professor Norio Shimizu and Yu Zhang of Chiba University. Cell lines were authenticated using Short Tandem Repeat (STR) analysis (Genetic Testing Biotechnology, STR Profile Reports in Supplemental Data). Recent mycoplasma testing has been performed with Lonza LT07-705 MycoAlert™ PLUS Mycoplasma Detection Kit. NK-92 cells were cultured in α -MEM medium supplemented with 10% FBS, 10% HBS and recombinant human IL-2 (20ng/ml). SNK-6 cells were cultured in RPMI-1640 medium supplemented with 10% FBS, 10% HBS and recombinant human IL-2 (80ng/ml). Asparaginase (Cat# A3809), 13 C-glutamine (Cat# 184161-19-1), and glutamine (Cat# 56-85-9) were obtained from Sigma-Aldrich (St.Louis, MO, USA). Anti-PD-1 antibody pembrolizumab (Cat# A2005) was from Selleck Chemicals (Houston, TX, USA).

2.7. Cell transfection

Cells were incubated overnight with viral particles containing purified plasmids pGV367-EGFP-*SLC1A1* vector, pGV367-EGFP-control vector, pGV358-EGFR-TP53-R248Q, pGV358-EGFR-TP53-R273H, pGV358-EGFP-control vector, pGV365-EGFR-EP300-WT, or pGV365-EGFP-control vector (MOI=50). The stably transfected clones were selected by Green Fluorescent Proteins (GFP). Cells were also transfected with MGA shRNA (Cat# TL317004, Origene, Rockville, MD, USA) or *SLC1A1* shRNA (Cat# TL309389, Origene) using Lipofectamine 3000 (Cat# L3000015, Invitrogen, Shanghai, China) transfection reagents, according to the manufacturer's instruction.

2.8. Analysis of 13 C-glutamine uptake and the derived metabolites by LC-MS/MS

To assess the glutamine uptake and glutamine-derived metabolites, cells were cultured in glutamine-free medium supplemented with 2 mM 13 C-glutamine (Sigma-Aldrich). After incubation for 24 hours, cell lysis was collected for metabolic analysis using an UHPLC system (1290, Agilent Technologies) with a UPLC HSS T3 column (2.1 mm×100 mm, 1.8 μ m) coupled to Q Exactive mass spectrometer (Thermo). The raw data were converted to the mzXML format using ProteoWizard and processed with an in-house program, which was developed using R and based on XCMS [23], for peak detection, extraction, alignment, and integration. In-house MS2 database (BiotreeDB, Shanghai, China) was applied in metabolite annotation.

2.9. Cell viability

Cells (2×10⁵/ml) were seeded in 96-well plates and incubated with indicated concentration of reagents. Cell growth was assessed by CCK8 (1:10, Cat# CK04, Dojindo, Kumamoto, Japan) and the absorbance was measured at 450nm by spectrophotometry. The percentage of cell growth inhibition was calculated as treated or transfected cells divided by untreated or non-transfected cells.

2.10. Colony formation

Cells were mixed with an equal volume of 0.7% soft agarose and then plated in 12-well plates and incubated for 14 days. Colony formation was calculated as count of colonies with diameter more than 0.1 mm.

2.11. Quantitative real-time PCR

Total mRNA was extracted using TRIzol reagent (Cat# 15596026, Invitrogen, Shanghai, China). Complementary DNA was synthesized using PrimeScript RT Reagent Kit with gDNA Eraser (Cat# RR047A, TaKaRa, Dalian, China). Quantitative real-time PCR was performed by SYBR Premix Ex TaqTM II (Cat# RR820A, TaKaRa) and ABI ViiA 7 (Applied Biosystems) with primers as follows: *SLC1A1* (Forward: 5'-TCGAGAACACAGCAACCTCT-3', Reverse: 5'-TCACCACCAGCACAA-TACCT-3'), *PD-L1* (Forward: 5'-GCTGCTTAATTGTCTATTGGGA -3', Reverse: 5'-AATTCGCTTGTAGTCGGCACC -3'), and *GAPDH* (Forward: 5'-GCTCATTCTCTGGTATGACAAAC-3', Reverse: 5'-CTGTGAGGAGGGGA-GATTCA-3') was used as an endogenous control.

2.12. In vitro co-culture system

Transwell cell culture chambers (8 μ M, Millipore Corporation, Billerica, MA, USA) were used for co-culture assay [24]. In the co-culture system, lymphoma cells were plated on the upper chamber, with immune cells on the lower chamber. Immune cells were peripheral blood mononuclear cells (PBMC) isolated from peripheral blood of healthy volunteers using Ficoll by density gradient centrifugation. As for recognition of NKTCL cells by T cells, the MHC genotype of NKTCL cell lines are common and the MHC typing of PBMCs is not necessary.

2.13. Multi-color flow cytometry

Multi-color flow cytometry was carried out to assess the growth and immune receptor expression of tumor cells and immune cells. Co-cultured PBMC and NK-92 or SNK-6 cells were stained with commercial antibodies Fixable Viability Stain 440UV (BD pharmingen Cat# 566332, RRID:AB_2869748), anti-CD45 (BD pharmingen Cat# 563792, RRID:AB_563792), anti-CD19 (BD pharmingen Cat# 555415, RRID: AB_398597), anti-CD3 (BD pharmingen Cat# 612940, RRID: AB_2870222), anti-CD4 (BD pharmingen Cat# 624298, special order), anti-CD8 (BD pharmingen Cat# 563919, RRID: AB_2722546), Ki-67 (BD pharmingen Cat# 558615, RRID: AB_647130), anti-PD-L1 (BD pharmingen Cat# 751185, RRID: AB_2875207), anti-TIM-3 (Thermo Fisher Scientific Cat# 35-3109-42, RRID: AB_2811801) and collected by BD FACSymphony A5.

2.14. Xenograft zebrafish models

Cells were stained with Dil (Cat# D3911, Vybrant; Molecular Probes, Invitrogen, 4 μ L/mL in 1 \times PBS) for 3 min followed by 10 min on ice darkness and washed with 1 \times PBS for 2 times. Dil-labeled cells were injected into the perivertebra space (PVS) of anesthetized 48hpf (hours post fertilization) larvae at indicated concentration. Xenografts were observed under fluorescence microscope at 24hpi (hours post injection). For treatment, cells were injected into the PVS of anesthetized 48hpf larvae and treatment started at 24hpi. Censor of sensitivity was death event of zebrafish in following 7 days. The concentration of asparaginase (0.5 IU/mL) was determined based on patient plasma concentration.

3. Statistical analysis

Comparisons of metabolites in NKTCL, PTCL and DLBCL were ascertained by Pearson's chi-square test. LASSO regression was used

to perform feature selection for identifying key amino acid transporter factor using metabolic and RNA-seq data. The Lambda parameter was determined by 10-fold cross-validation with squared-error. As for metabolic analysis, LASSO regression was performed based on the principal component analysis of three metabolites (glutamate, glutamine, and aspartate). The coefficients of variables were calculated by fitting a general linear model of Gaussian distribution with quantitative dependent variable. R package glmnet (v4.0-2) [25] was executed for LASSO regression analysis. Progression-free survival (PFS) was calculated from the date when treatment began to the date when disease progression was recognized or the date of the last follow-up. Overall survival (OS) was measured from the date of diagnosis to the date of death or the last follow-up. Survival functions were estimated with Kaplan-Meier method and compared by log-rank test. Univariate hazard was estimated using unadjusted Cox proportional hazards models. Covariates demonstrating significance on univariate analysis were included in multivariate model. All survival analysis was performed using R (v3.5.0) or Statistical Package for the Social Sciences (SPSS) 20.0 software (SPSS Inc., Chicago, IL). $P < 0.05$ was considered statistically significant.

4. Role of funders

The Funders had no role in study design, data collection, data analyses, interpretation, or writing of manuscript.

5. Results

Serum metabolomic profile revealed aberrant glutamine metabolism in patients with NKTCL.

Serum metabolomic profile of NKTCL (n=36), PTCL (n=34), and DLBCL (n=33) were assessed by LC-MS and identified 146, 120 and 167 distinguished metabolites of amino acids, nucleotides, carbohydrates, and lipids, respectively (variable importance in projection > 1, $P < 0.05$ comparing with healthy volunteers, n=64, Table S1). Aforementioned metabolites were illustrated in the overview of metabolism network (Fig. 1a) using Interactive Pathways Explorer v3 (iPath 3, <https://pathways.embl.de>), showing that distinguished metabolites of NKTCL (red dots) were mainly enriched in metabolic pathways involving amino acids metabolism (yellow lines), while PTCL (dark blue dots) and DLBCL (light blue dots) in metabolic pathways involving lipids metabolism (green lines). Indeed, percentage of distinguished amino acid associated metabolites was significantly higher in NKTCL (29/146, 19.86%, Fig. 1b) than in PTCL (10/120, 8.33%, $P = 0.010$, chi-square test) and in DLBCL (20/167, 11.98%, $P = 0.022$, chi-square test), underlying a distinct metabolomic profile of NKTCL with featured changes in amino acid metabolism. This was further revealed by Kyoto Encyclopedia of Genes and Genomes (KEGG, <http://www.kegg.jp>) pathway enrichment (Table S2) using ConsensusPathDB (<http://cpdb.molgen.mpg.de>). Aminoacyl-tRNA biosynthesis was the most significantly altered metabolic pathway in NKTCL, and 8 out of 15 enriched metabolism pathways ($P < 0.01$) were related to amino acid metabolism (Fig. 1c). Moreover, 14 out of 20 standard amino acids were significantly upregulated in NKTCL (Fig. 1d). Among them, glutamate, glutamine, and aspartate were the top three altered amino acids, indicating a major role of altered glutaminolysis in patients with NKTCL.

5.1. SLC1A1 enhanced cellular glutamine uptake and had increased expression in patients with NKTCL

Among the 65 SLC families of transporters, 26 transporters were responsible for amino acid transportation (Table S3) [12]. To determine the key transporter affecting altered glutaminolysis in NKTCL, quantification of 20 standard amino acids (Table S4) was performed using previously designed targeted metabolic analysis protocol [6] in

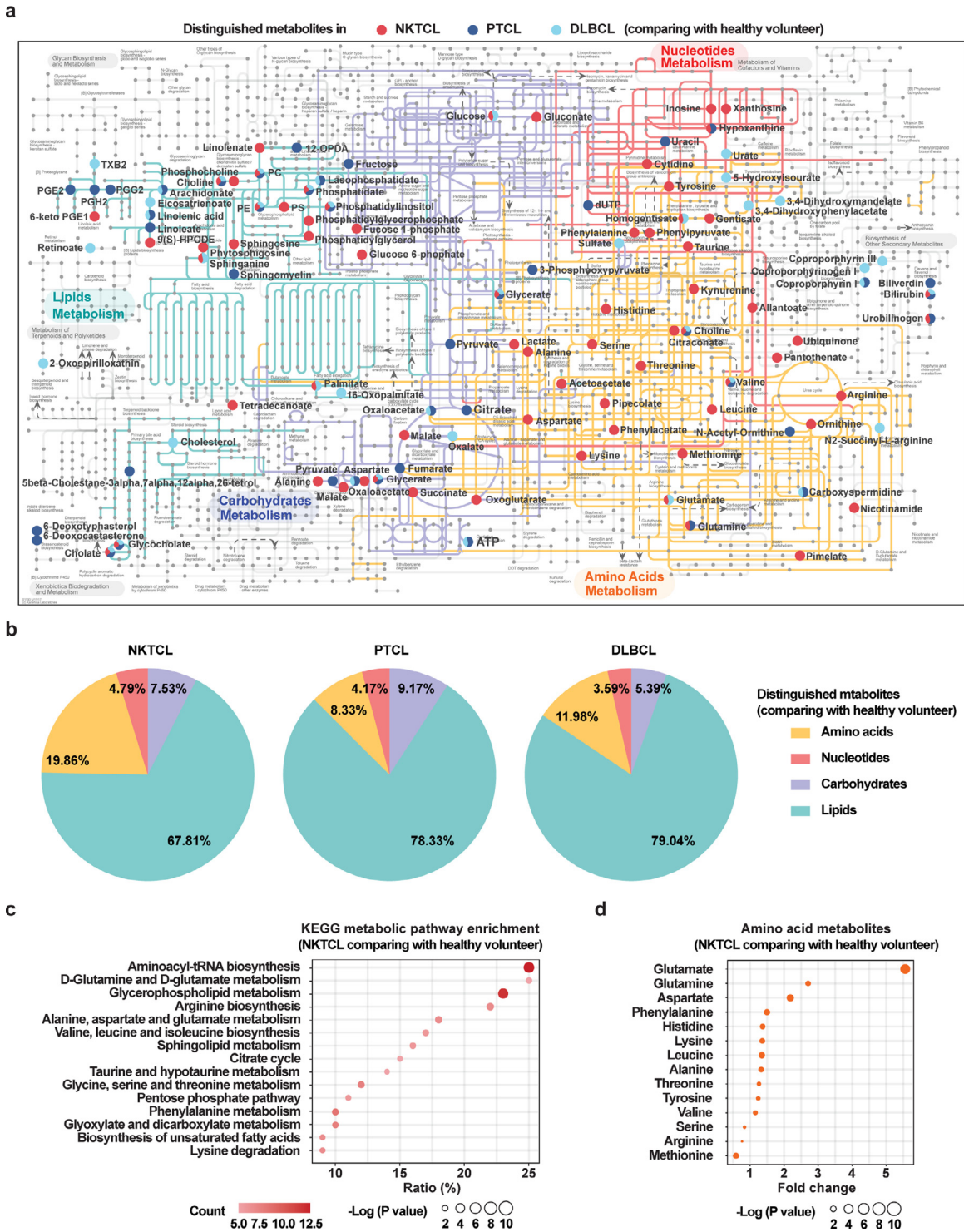


Fig. 1. Metabolomic assay indicated aberrant glutamine metabolism in patients with NKTC.

(a) Distinguished serum metabolites of NKTC (red dots), PTCL (dark blue dots), and DLBCL (light blue dots), comparing with healthy volunteer, were overlaid on human metabolic reference map (KEGG: hsa01100) using Interactive Pathways Explorer v3 (iPath 3). Pathways involving amino acid metabolism (yellow lines), nucleotide metabolism (red lines), carbohydrate metabolism (purple lines) and lipid metabolism (green lines) were highlighted.

(b) Distinguished serum metabolites of NKTC, PTCL and DLBCL, comparing with healthy volunteer, were categorized into 4 subtypes according to their relevance to amino acid, nucleotide, carbohydrate, or lipid metabolism.

(c) KEGG metabolic pathway enrichment by ConsensusPathDB using distinguished serum metabolites of NKTC, comparing with healthy volunteer.

(d) Standard amino acids significantly altered in NKTC, comparing with healthy volunteer.

102 NKTC patients with available serum samples. A three-metabolite (glutamate, glutamine, and aspartate) model was developed using LASSO regression on data from targeted serum metabolic analysis and paired tumor RNA-seq data (detailed in Mendeley dataset).

With the lambda at minimum mean-squared error in 10-fold cross validation (Fig. 2a), *SLC1A1* was screened out by the highest coefficient (0.724), while the coefficient of the remaining genes converged to zero (Fig. 2b). *SLC1A1* encodes the excitatory amino acid

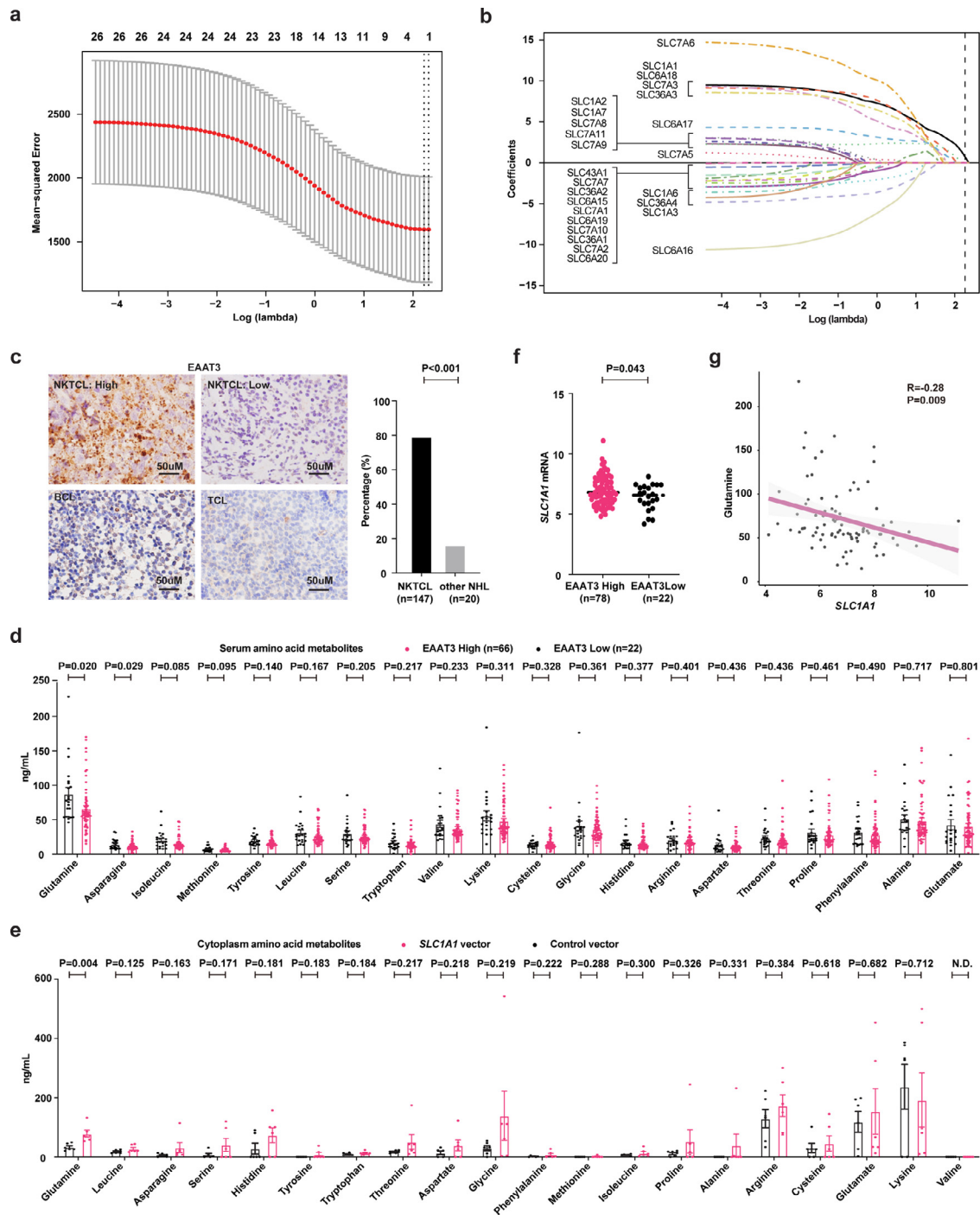


Fig. 2. SLC1A1 enhanced glutamine uptake and was highly expressed in patients with NKTL.

(a) LASSO regression analysis in 10-fold cross-validation was performed with selected metabolites (glutamate, glutamine, and aspartate). Two dotted vertical lines marked the lambda at minimum and 1-s.e. mean-squared error, respectively.

(b) LASSO coefficient profiles of 26 SLC-family genes. A vertical line indicated the value of lambda at minimum mean-squared error.

(c) Tumor EAAT3 expression detected by immunohistochemistry.

(d) Quantification of targeted amino acids (arranged by P values from left to right) in serum samples of NKTL patients (n=88) according to tumor EAAT3 expression.

(e) Quantification of targeted amino acids (arranged by P values from left to right) in cytoplasm samples of NK-92 cells transfected with SLC1A1 vector or control vector.

(f) Tumor EAAT3 expression correlated with its mRNA levels in NKTL patients (n=100).

(g) Correlation of tumor SLC1A1 mRNA expression with serum glutamine levels in NKTL patients (n=102).

Assays in (e) were set up in 6 replicated. Data in (d), (e) and (f) were represented as mean \pm SD. P values in (c) were calculated by Pearson's chi-square test. P values in (d), (e) and (f) were calculated with unpaired t-test. P value in (g) was calculated by Pearson correlation test.

transporter EAAT3 and is essential in glutamate transport across cell membrane [26]. Immunohistochemistry of tumor EAAT3 expression, which is more feasible in clinical practice, was then performed in 100 NKTL patients with available paraffin sections. High EAAT3 expression (immunoreactive score ≥ 4 , representative images in Fig. 2c) was

observed in 117 of 147 (80%) NKTL patients ($P < 0.001$, chi-square test, comparing with 15% in other types of lymphoma). To identify the key metabolite in SLC1A1/EAAT3-mediated amino acid metabolic alteration, we performed quantification of 20 targeted amino acids both in serum samples of NKTL patients and in NK-92 cells. As for

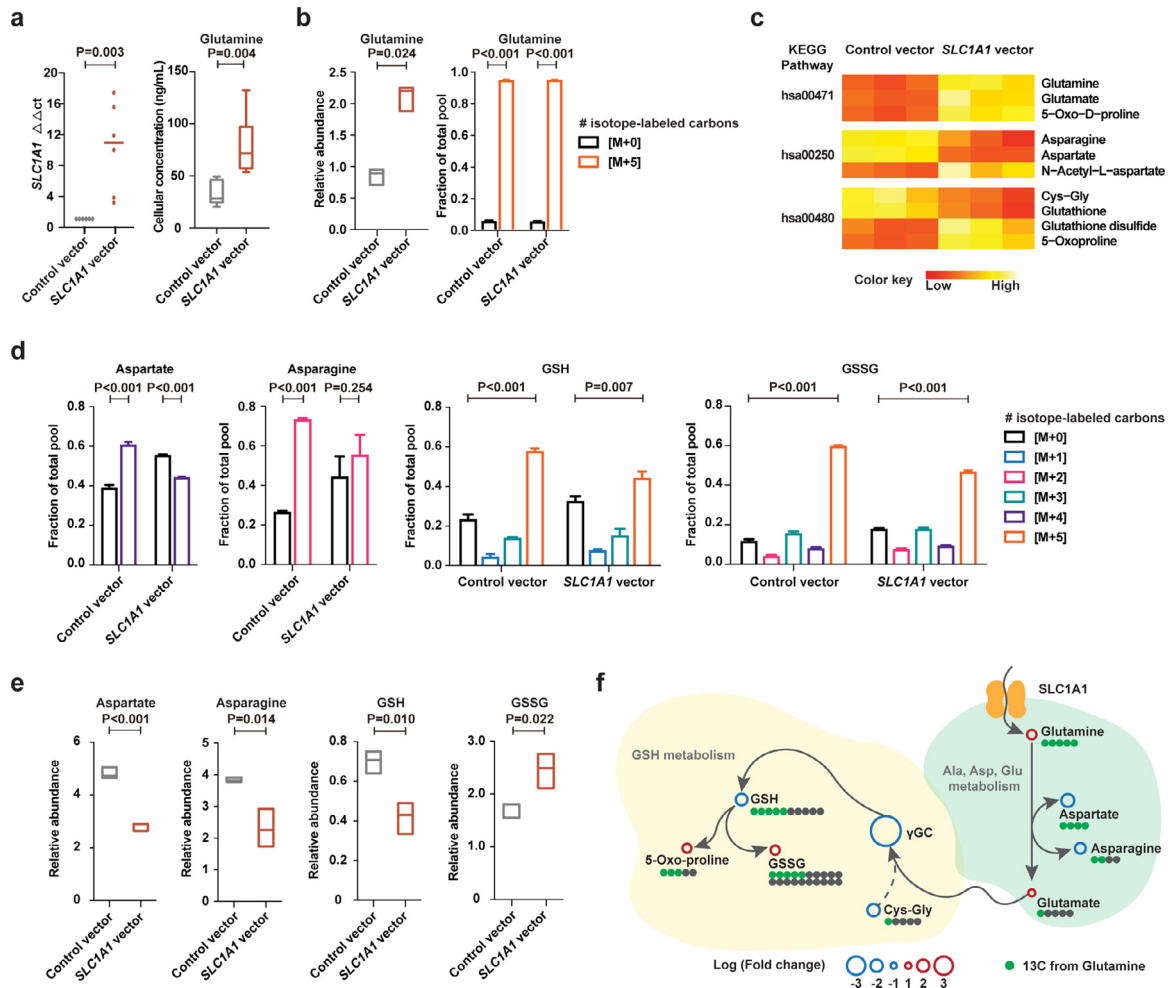


Fig. 3. Increased glutamine uptake mediated by SLC1A1 enhanced glutathione metabolic flux.

(a) SLC1A1 mRNA expression (left panel) and cellular glutamine levels (right panel) in NK-92 cells transfected with SLC1A1 vector or control vector. The control vector values of SLC1A1 mRNA expression were normalized to 1.

(b) Relative abundance (left panel) and isotope-labeled fraction (right panel) of glutamine in NK-92 cells transfected with SLC1A1 vector or control vector.

(c) Heatmaps of isotope-labeled metabolites significantly altered in NK-92 cells transfected with SLC1A1 vector, comparing with control vector. The aberrant metabolites were enriched into the KEGG pathways indicated at left: hsa00471, D-glutamine and D-glutamate metabolism; hsa00250, alanine, aspartate and glutamate metabolism; hsa00480, glutathione metabolism.

(d and e) The isotope-labeled fraction (d) and relative abundance (e) of aspartate, asparagine, GSH, and GSSG in NK-92 cells transfected with SLC1A1 vector or control vector.

(f) A schematic to show the metabolic flux of isotope-labeled glutamine.

Assays in (a, right panel) were set up in 6 replications. Assays in (b), (d) and (e) were set up in triplicate. Data in (a), (b), (d) and (e) were represented as mean \pm SD. P values in (a), (b), (d) and (e) were calculated with unpaired t-test.

serum metabolites quantification, glutamine and asparagine were significantly decreased in NKTCL patients with high EAAT3 expression group, as compared to low EAAT3 expression group (Fig. 2d). As for cytoplasm metabolites quantification of NK-92 cells, glutamine was significantly increased in NK-92 cells transfected with SLC1A1 vector, as compared to control vector (Fig. 2e). Also confirmed in transcriptional levels assessed by RNA-seq, tumor SLC1A1 mRNA level was significantly correlated with protein expression (Fig. 2f), and negatively correlated with serum glutamine (Fig. 2g). Therefore, SLC1A1/EAAT3 was overexpressed and enhanced cellular glutamine uptake, leading to altered glutaminolysis in patients with NKTCL.

5.2. SLC1A1 enhanced glutathione metabolic flux and mediated glutamine addiction

Glutamine belongs to a group of conditionally essential amino acids, providing carbon and nitrogen source to support biosynthesis, energetics and cellular homeostasis that necessary for tumor growth [27]. NK-92 is the only commercially available NK phenotype (CD3-/

CD4-/CD8-/CD56+/TCR-) cell line without STAT3-activating mutations (Table S5) [28–30]. To determine the biological function of SLC1A1 on altered glutaminolysis in NKTCL, NK-92 cells were transfected with SLC1A1 vector or control vector (Fig. 3a, left panel). Cellular glutamine uptake was significantly increased by ectopic expression of SLC1A1 (Fig. 3a, right panel). Metabolic flux assay was further performed using ^{13}C -glutamine to trace glutamine utilization. Cells were cultured in 2 mM ^{13}C -glutamine (C5H10N2O3 [M+5], MW146.0691) for 24 hours and then cell lysates were collected for analysis. SLC1A1-transfected NK-92 cells displayed significantly higher ^{13}C -glutamine uptake than those transfected with control vector, mainly as isotope-labeled glutamine (Fig. 3b). Among 345 isotope-labeled metabolites filtered by KEGG database (Table S6), 94 metabolites revealed significant changes of relative abundance in SLC1A1-transfected NK-92 cells, and enriched in metabolism pathways, namely D-Glutamine and D-glutamate metabolism (KEGG: hsa00471), alanine, aspartate and glutamate metabolism (KEGG: hsa00250), and glutathione metabolism (KEGG: hsa00480) (Fig. 3c; Table S7). The metabolic flux of glutamine was traced by calculating

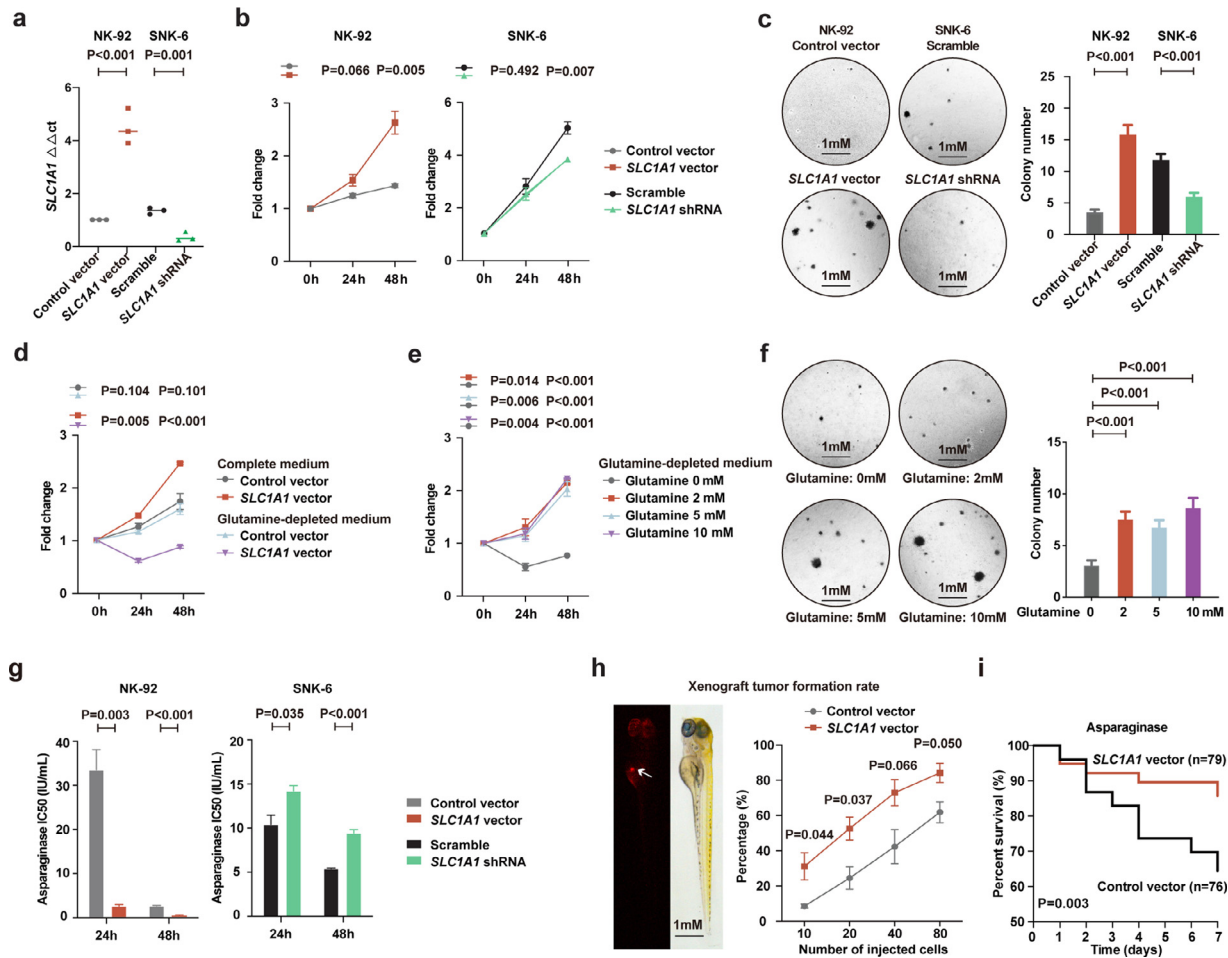


Fig. 4. SLC1A1-mediated glutamine addition and malignant phenotype in NKTCL.

(a, b, and c) SLC1A1 expression (a), cell proliferation (b) and colony formation (c) of NK-92 cells transfected with SLC1A1 vector or control vector and SNK-6 cells transfected with SLC1A1 shRNA or scramble.

(d) Cell viability of NK-92 cells transfected with SLC1A1 vector or control vector under glutamine-depleted medium.

(e and f) Cell growth inhibition (e) and colony formation (f) of NK-92 cells transfected with SLC1A1 vector under indicated culture medium.

(g) IC50 of NK-92 cells transfected with SLC1A1 vector or control vector and SNK-6 cells transfected with SLC1A1 shRNA or scramble treated with asparaginase.

(h) Tumor formation of NK-92 cells transfected with SLC1A1 vector or control vector under indicated number of injected cells in xenograft zebrafish models.

(i) Survival of xenograft zebrafish models injected with NK-92 cells transfected with SLC1A1 vector or control vector upon asparaginase treatment (0.5 IU/mL).

All the assays were set up in triplicate. Data in (a), (b), (c), (d), (e), (f), (g) and (h) were represented as mean \pm SD. P values in (a), (b), (c), (d), (e), (f), (g) and (h) were calculated with unpaired t-test. P values in (i) were calculated with log-rank test.

the fraction of isotope-labeled carbons in total pool. Isotope-labeled aspartate (M+4), asparagine (M+2), glutathione (GSH, M+5), glutathione disulfide (GSSG, M+5) represented the main forms of metabolites (Fig. 3d), suggesting that uptake of extracellular glutamine may serve as the carbon source for aspartate/asparagine and GSH/GSSG metabolism. As for relative abundance, increased metabolic end-product GSSG, while decreased upstream metabolic intermediates aspartate, asparagine, and GSH, were observed in SLC1A1-transfected NK-92 cells (Fig. 3e). Together, SLC1A1 enhanced cellular glutamine uptake and regulated glutathione metabolism in NKTCL (Fig. 3f).

Meanwhile, low expression of ASNS was observed in 58 of the 68 NKTCL patients (85%) as assessed by immunohistochemistry (Fig. S2a) and negatively correlated with prognosis of asparaginase-treated patients (Fig. S2b) [8]. In according with the metabolic flux assay, EAAT3-transported glutamine was the major source for glutathione metabolism rather than ASNS-catalyzed synthesis of asparagine.

5.3. Asparaginase counteracted SLC1A1-mediated glutamine addiction and tumor cell proliferation in NKTCL

Altered glutaminolysis may exacerbate malignant phenotypes in cancers [31]. Ectopic expression or molecular silencing of SLC1A1 was

induced by transfecting with SLC1A1 vector or SLC1A1 shRNA in NK-92 and SNK-6 cells, respectively (Fig. 4a). Indeed, SLC1A1 remarkably accelerated cell proliferation (Fig. 4b) and promoted colony formation (Fig. 4c). Glutamine addition in SLC1A1-transfected NK-92 cells was further demonstrated by cell viability, which was reduced when cultured in medium lack of glutamine and interlinked asparagine (Fig. 4d), but rescued by the addition of glutamine (Fig. 4e). Similar results were obtained for colony formation assay (Fig. 4f). Together, these data confirmed that SLC1A1 acted as an extracellular glutamine transporter, promoting tumor cell proliferation through reprogramming glutamine metabolism in NKTCL.

Asparaginase is a key anti-metabolic agent to treat NKTCL, exerting therapeutic effect through depleting extracellular asparagine and inhibiting glutamine-dependent tumor cell growth [32]. SLC1A1-overexpressing NK-92 cells were more sensitive to asparaginase than those transfected with control vector (24h IC50: 2.48 vs 33.40 IU/mL, $P=0.003$, 48h IC50: 0.36 vs 2.54 IU/mL, $P<0.001$, unpaired t-test, Fig. 4g, left panel). SLC1A1-downregulating SNK-6 cells were less sensitive to asparaginase than those transfected with scramble (24h IC50: 14.23 vs 10.45 IU/mL, $P=0.035$, 48h IC50: 9.45 vs 5.43 IU/mL, $P<0.001$, unpaired t-test, Fig. 4g, right panel). Similar results were observed upon treatment with glutamine inhibitor BPTES. SLC1A1-

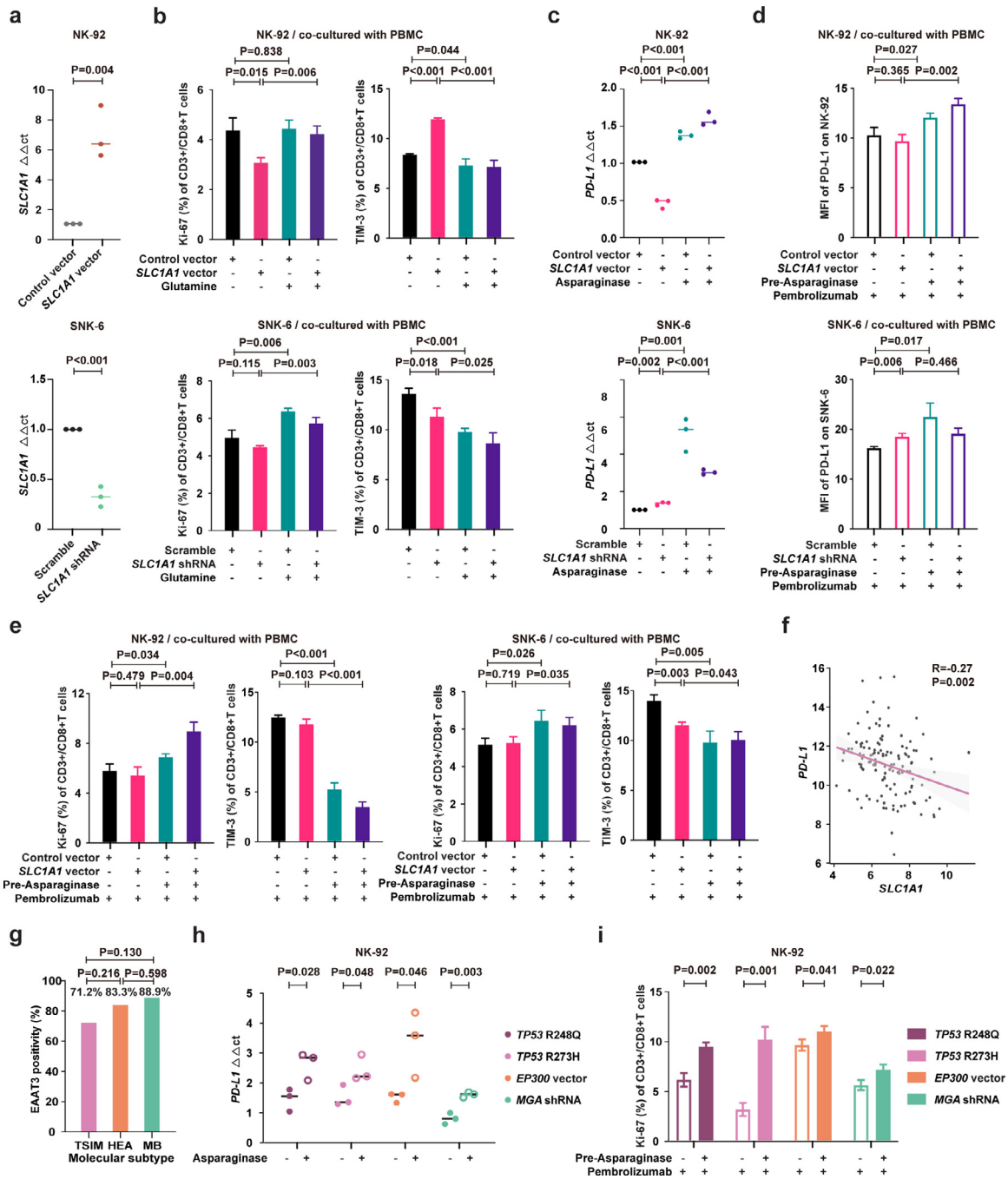


Fig. 5. Asparaginase treatment increased NK-TCL cell sensitivity to anti-PD-1 antibody.

(a) SLC1A1 expression on NK-92 cells transfected with SLC1A1 vector or control vector (upper panel) and SNK-6 cells transfected with SLC1A1 shRNA or scramble (lower panel). (b) Ki-67 and TIM-3 positivity of CD3+/CD8+ T cells in PBMC co-cultured with NK-92 cells (upper panel) or SNK-6 cells (lower panel) transfected with indicated vectors or shRNAs in medium with or without extra glutamine (2mM). (c) PD-L1 mRNA expression in NK-92 cells transfected with SLC1A1 vector or control vector (upper panel) and SNK-6 cells transfected with SLC1A1 shRNA or scramble (lower panel) upon asparaginase (10 IU/mL) treatment. The control vector or scramble values were normalized to 1, respectively. (d and e) Median fluorescence intensity of PD-L1 (d) on NK-92 cells (upper panel) or SNK-6 cells (lower panel), as well as Ki-67 and TIM-3 positivity of CD3+/CD8+ T cells in PBMC co-cultured with NK-92 cells (upper panel) or SNK-6 cells (lower panel) upon indicated treatment. (f) Gene expression correlation of tumor SLC1A1 with PD-L1 in NK-TCL patients ($n=128$). (g) Tumor EAAT3 expression according to the TSIM, HEA, and MB subtypes in NK-TCL patients ($n=100$). (h) PD-L1 mRNA expression of NK-92 cells transfected with TP53 R248Q, TP53 R273H, EP300 vector, or MGA shRNA upon indicated treatment. (i) Ki-67 positivity of CD3+/CD8+ T cells in PBMC co-cultured with NK-92 cells transfected with TP53 R248Q, TP53 R273H, EP300 vector, or MGA shRNA upon indicated treatment.

Assays in (a), (b), (c), (d), (e), (h), and (i) were set up in triplicate. Data in (a), (b), (c), (d), (e), (h), and (i) were represented as mean \pm SD. P values in (a), (b), (c), (d), (e), (h), and (i) were calculated with unpaired t-test. P value in (f) was calculated with Pearson correlation test. P values in (g) were calculated by Pearson's chi-square test.

overexpressing NK-92 cells were more sensitive to BPTES than those transfected with control vector (24h IC50: 56.33 vs 123.40 mM, $P < 0.001$, 48h IC50: 41.67 vs 91.12 mM, $P = 0.004$, unpaired t-test, Fig. S3, left panel). *SLC1A1*-downregulating SNK-6 cells were less sensitive to BPTES than those transfected with scramble (24h IC50: 160.27 vs 128.25 mM, $P = 0.011$, 48h IC50: 74.79 vs 25.03 mM, $P < 0.001$, unpaired t-test, Fig. S3, right panel). Meanwhile, zebrafish xenograft models injected with NK-92 cells bearing ectopic expression of *SLC1A1* also presented enhanced xenograft tumor formation rate (Fig. 4h) and prolonged survival time upon asparaginase treatment (Fig. 4i). Therefore, dependence of extracellular glutamine induced by *SLC1A1* on NKTCL cells were overcome by asparaginase treatment both *in vitro* and *in vivo*, suggestive a potential mechanism of targeting metabolic vulnerabilities in NKTCL.

5.4. Asparaginase restored *SLC1A1*-induced impaired T-cell immunity and sensitized tumor cells to anti-PD-1 antibody

Glutamine metabolism can modulate immunological states in cancers [33]. To mimic *in vivo* situation, NK-92 or SNK-6 cells were

co-cultured with PBMC. Ectopic expression of *SLC1A1* was induced in NK-92 cells transfected with *SLC1A1* vector (Fig. 5a, upper panel) and molecular silencing of *SLC1A1* was induced in SNK-6 cells transfected with *SLC1A1* shRNA (Fig. 5a, lower panel). Tumor cells avidly consume and compete T cells for amino acids by overexpressing amino acid transporter [34]. As revealed by multi-color flow cytometry, high *SLC1A1* (NK-92 cells transfected with *SLC1A1* vector, or SNK-6 cells transfected with scramble) provoked significantly decreased Ki-67 and increased TIM-3 expression on CD3+/CD8+ T cells, as compared to those with low *SLC1A1* (NK-92 cells transfected with control vector, or SNK-6 cells transfected with *SLC1A1* shRNA), respectively (Fig. 5b), indicating that *SLC1A1* overexpression impaired cytotoxic T-cell function. To demonstrate the relevance of glutamine competition between tumor cells and T cells, complementary study was performed and showed that the addition of glutamine (2 mM) restored CD3+/CD8+ T cell function by increasing Ki-67 and decreasing TIM-3 expression (Fig. 5b). No significant change was observed in CD3+/CD4+ T cells (Fig. S4). NK-92 cells transfected with *SLC1A1* vector showed lower *PD-L1* level than those transfected with control vector and SNK-6 cells transfected with shRNA *SLC1A1* showed higher *PD-L1*

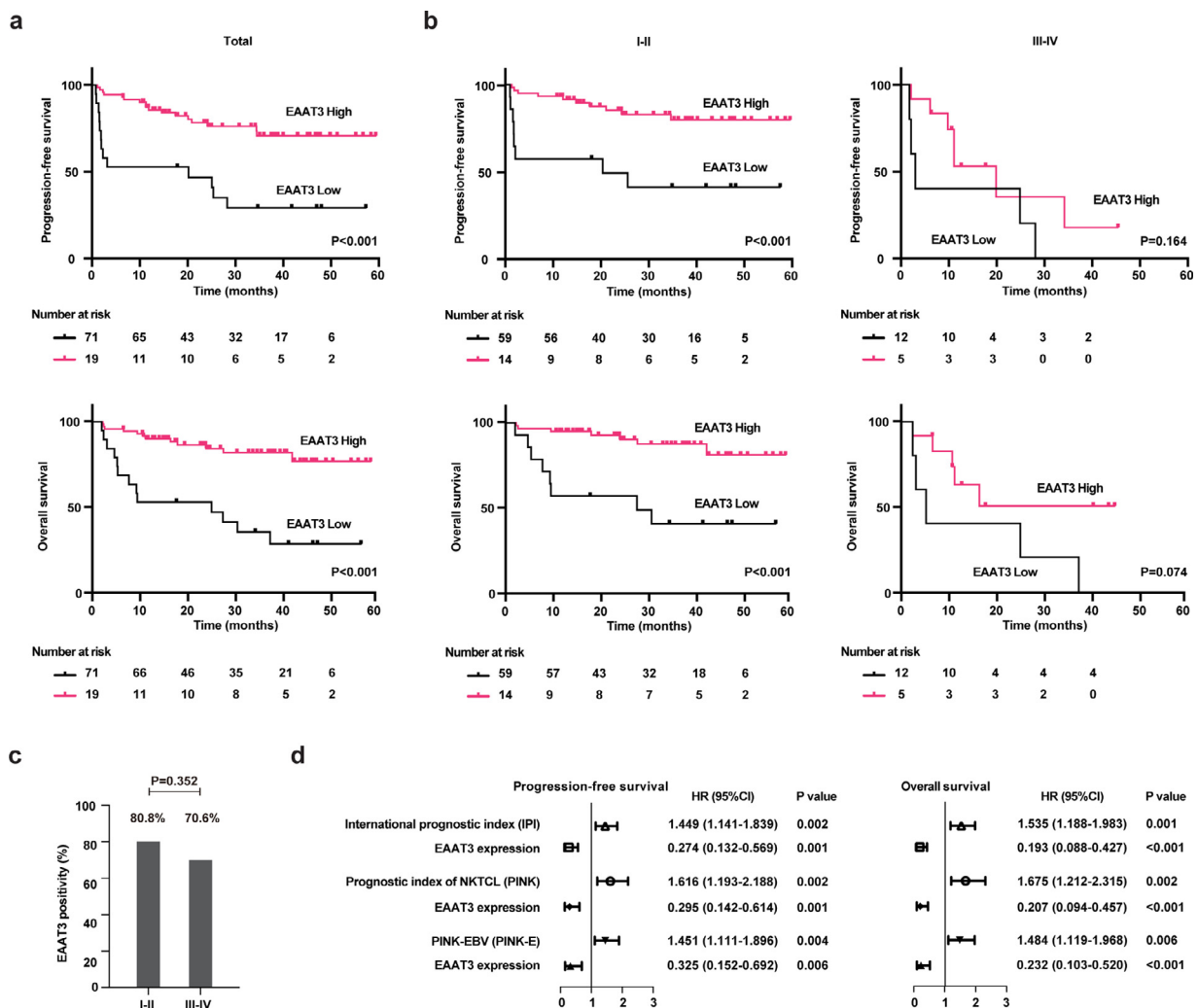


Fig. 6. Clinical outcome according to EAAT3 expression in patients with NKTCL.

(a and b) Progression-free survival (PFS, upper panel) and overall survival (OS, lower panel) according to tumor EAAT3 expression in all the patients (a), and stage I-II or III-IV patients (b) treated with asparaginase-based regimens.

(c) Tumor EAAT3 expression in stage I-II or III-IV patients.

(d) Multivariate analysis of predictors indicated on the left (EAAT3 and IPI, EAAT3 and PINK, or EAAT3 and PINK-E) for PFS and OS in NKTCL. Hazard ratio (HR), 95% confidence interval (95% CI) and P value were indicated on the right of each forest plot.

P values in (a) and (b) were calculated with log-rank test. P value in (c) was calculated with Pearson's chi-square test. P values in (d) was calculated with Cox proportional hazards models.

level than those transfected with scramble, both of which were upregulated by asparaginase (10 IU/mL) (Fig. 5c), underlying an alternative mechanism of tumor escape from immune surveillance. Moreover, when treated with anti-PD-1 antibody pembrolizumab, NK-92 and SNK-6 cells pretreated with asparaginase (10 IU/mL, 24h) elicited significantly increased expression of PD-L1 of NKTCL cells (Fig. 5d), increased Ki-67, but decreased TIM-3 expression of CD3+/CD8+ T cells in PBMC (Fig. 5e), as compared to untreated cells in co-culturing systems. *SLC1A1* (chr9: 4,490,427-4,587,469) was located at the same chromosome segment of *JAK2* (chr9: 4,984,390-5,129,948) and *PD-L1* (also known as *CD274*, chr9: 5,450,503-5,470,567). A negative correlation between *SLC1A1* and *PD-L1* was observed (Fig. 5f). Based on the fact that JAK-STAT pathway molecules (*JAK2*, *JAK3*, *STAT3*, *STAT5A*, and *STAT5B*) frequently mutated in NKTCL [5] may also affect cytotoxic T-cell proliferation [35] and tumor *PD-L1* expression [30], expression levels of JAK-STAT pathway molecules were also assessed by RNA-seq data (Fig. S5).

Expression levels of tumor EAAT3 were comparable across the TSIM (71.2%, 37/52), HEA (83.3%, 25/30), and MB subtypes (88.9%, 16/18, Fig. 5g) in NKTCL patients. NK-92 cell models were established as our previous study described [5], representing three molecular subtypes of NKTCL, including TSIM-like: *TP53* R248Q, *TP53* R273H, HEA-like: *EP300* vector; MB-like: *MGA* shRNA). When treated with anti-PD-1 antibody pembrolizumab, pretreatment of asparaginase upregulated NKTCL cellular *PD-L1* expression (Fig. 5h) and increased ki-67 expression of CD3+/CD8+ T cells (Fig. 5i) in the TSIM, HEA, or MB cell models, indicating anti-metabolic treatment also induced therapeutic vulnerability for immune checkpoint inhibitor.

5.5. Higher expression of EAAT3 independently predicted favorable clinical outcomes in NKTCL patients treated with asparaginase-based regimens

Clinical efficacy of EAAT3 was evaluated, indicating relatively poor clinical outcome in NKTCL patients receiving CHOP/CHOP-like regimens (Fig. S6). As for asparaginase-based regimens, significantly improved overall response rate (88.7% vs 45.5%) and complete remission rate (85.9% vs 45.5%) were revealed in patients with high EAAT3 expression than those with low EAAT3 expression, while other baseline clinical characteristics were comparable (Table 1). Prolonged PFS (median follow-up: 24.3 months, predicted 2-year PFS rates: 78.3% vs 46.8%) and OS (median follow-up: 27.4 months, predicted 2-year OS rates: 86.3% vs 52.6%) were also observed in patients with high EAAT3 expression, as compared to those with low EAAT3 expression (Fig. 6a). Particularly, high EAAT3 expression was associated with favorable clinical outcome in stage I-II patients (Fig. 6b). Although expression levels of EAAT3 were comparable between stage I-II (80.8%, 59/73) and stage III-IV patients (70.6%, 12/17, Fig. 6c), stage I-II patients with low EAAT3 expression presented similar inferior prognosis as stage III-IV patients (predicted 2-year PFS rates: 49.0% vs 39.9%, $P=0.537$, log-rank test; predicted 2-year OS rates: 57.1% vs 48.6%, $P=0.796$, log-rank test). In multivariate analysis, when international prognostic index (IPI), prognostic index of NKTCL (PINK), or PINK-EBV (PINK-E) [36] was controlled, EAAT3 was an independent prognostic factor for better PFS and OS (Fig. 6d).

6. Discussion

Growing evidence indicates a pivotal effect of aberrant glutamine metabolism on lymphoma progression and therapeutic resistance. In DLBCL, enhanced glutamine utilization is induced by SIRT3, which provokes B-cell lymphomagenesis through a metabolic-provoked non-oncogene mechanism [37]. Mitochondrial-targeted class I sirtuin inhibitor YC8-02 interrupts glutamine utilization and induces DLBCL cell death [37]. In mantle cell lymphoma, altered glutaminolysis has also been found and linked to therapeutic resistance to the Bruton's

tyrosine kinase inhibitor ibrutinib [38]. IACS-010759 targets complex I of the mitochondrial electron transport chain and results in marked growth inhibition in ibrutinib-resistant patient-derived tumor models [38]. The SLC-family amino acid transporters are responsible for increased cellular glutamine uptake, such as *SLC1A5* [38], *SLC38A1* [39], and *SLC1A1* [40]. *SLC1A5*, acting upstream of mTOR and MYC signaling, is upregulated in ibrutinib-resistant mantle cell lymphoma [38]. *SLC38A1* expression is an independent adverse prognostic factor of acute myeloid leukemia [41]. Here we revealed distinct feature of aberrant glutamine metabolism in NKTCL and identified *SLC1A1* as key inducer of glutamine addiction. *SLC1A1* enhanced glutamine utilization, activated glutathione metabolic flux, and consequently increased GSSG production. In NK-92 cells and xenograft models, *SLC1A1*-induced altered glutaminolysis was involved in tumor cell proliferation and colony formation, exacerbating malignant phenotypes in NKTCL.

SLC1A1 induced dependence of tumor cells on extracellular glutamine, suggestive an alternative mechanism of metabolic reprogramming on lymphoma progression, and a potential therapeutic target of asparaginase in NKTCL. Asparaginase exerted anti-metabolic effect through depleting extracellular asparagine and inhibiting glutamine-dependent tumor cell growth [42]. *SLC1A1*-overexpressed tumor cells revealed increased sensitivity to asparaginase both in vitro and in vivo. In NKTCL patients treated with asparaginase-based regimens, prognostic analysis further indicated correlation of high EAAT3 expression with good clinical response to asparaginase treatment. Stage I-II NKTCL usually presents with favorable clinical outcome upon anti-metabolic treatment combined with local radiotherapy. However, prognosis of stage I-II patients with low EAAT3 expression was not only worse than those with high EAAT3 expression, but also as poor as stage III-IV patients, pointing out the necessity for this subset of NKTCL patients to receive molecular subtype-specific targeted therapy.

Cancer metabolism can modulate immune cell function and recent studies have focused on the role of amino acid metabolism in T-cell activation [43]. Glutamine is exploited as a "metabolic checkpoint" by inducing divergent metabolic plasticity between cancer cells and effector T cells [44]. For example, *SLC43A2* overexpression outcompetes for methionine in tumor microenvironment, reducing *STAT5* expression and contributing to impaired T-cell survival and function [34]. Oncogenic *JAK2* mutation affects methionine and cysteine metabolism in T cells [45], upregulates *PD-L1* expression, and promotes tumor cell response to PD-1 blockade [46]. Here we found a competition for glutamine between *SLC1A1*-overexpressed tumor cells and co-cultured CD8+ T cells. Asparaginase, therapeutically targeting *SLC1A1*-mediated glutamine addiction, induced tumoral *PD-L1* expression and modulated CD8+ T cell activity, potentially sensitized NKTCL cells to anti-PD-1 antibody pembrolizumab. Similar results have been recently reported in renal cancer [33] and lung cancer [47], revealing that tumor *PD-L1* expression is increased during glutamine deprivation [33] and inhibition of glutamine metabolism and immune checkpoint augmented CD8+ T cell-mediated anti-tumor immunity [47]. We hypothesized that co-targeting metabolic vulnerability alterations and immune checkpoints could be a promising therapeutic strategy in treating NKTCL. Further studies will be carried out to investigate the molecular mechanism of metabolism-regulated tumor immunity, as well as validate the efficacy of co-targeting metabolism and immunity in clinical trials.

In conclusion, *SLC1A1* mediated aberrant glutamine metabolism in NKTCL and was closely related to tumor progression and immunosuppressive status. Our findings indicated *SLC1A1* as a potential therapeutic target of NKTCL in the era of asparaginase-based anti-metabolic treatment, and might provide clinical rationale for co-targeting metabolic vulnerability and immunosuppressive microenvironment in NKTCL.

Contributors

J.X. and N.W. performed experiments and carried out clinical analysis. H.-J.Z. and S.C. gathered detailed clinical information. B.-W.C. and J.-Y.H. were responsible for bioinformatics investigation. S.R., J.-Y.C., G.C., P.-P.X., L.W., X.-J. S., and J.-Y.H. gave technical support. W.-L.Z. conceived the study, directed and supervised research, and wrote the manuscript. J.X., N.W., B.-W.C., H.-J.Z. and W.-L.Z. verified the underlying data. All authors read and approved the final version of the manuscript.

Declaration of Competing Interest

None.

Acknowledgments

This study was supported, in part, by research funding from the National Natural Science Foundation of China (82130004, 81830007 and 81900192), Chang Jiang Scholars Program, Shanghai Municipal Education Commission Gaofeng Clinical Medicine Grant Support (20152206 and 20152208), Clinical Research Plan of SHDC (2020CR1032B), Multicenter Clinical Research Project by Shanghai Jiao Tong University School of Medicine (DLY201601), Shanghai Chenguang Program (19CG15), Shanghai Sailing Program (19YF1430800), Medical-Engineering Cross Foundation of Shanghai Jiao Tong University (ZH2018QNA46), and Shanghai Yi Yuan Xin Xing Program. We thank multi-center Hematology-Oncology Protocols Evaluation System (M-HOPES) network from China, Collaborative Innovation Center of Systems Biomedicine, Samuel Waxman Cancer Research Foundation, and the Center for High Performance Computing at Shanghai Jiao Tong University.

Data sharing statement

RNA-seq data can be viewed in NODE (<http://www.biosino.org/node>) by pasting the accession OEP000498) into the text search box or through the URL: <http://www.biosino.org/node/project/detail/OEP000498>. The detailed RNA-seq expression data can be downloaded from the Mendeley Dataset, accessible through the following link: https://data.mendeley.com/datasets/mck239rj7k/draft?_a=9602c066-5331-4c8c-bcd6-c12b65939011. All data are available without any restrictions. Correspondence and requests for materials should be addressed to W.-L.Z.

Supplementary materials

Supplementary material associated with this article can be found, in the online version, at [doi:10.1016/j.ebiom.2021.103614](https://doi.org/10.1016/j.ebiom.2021.103614).

Reference

- Tse E, Kwong Y-L. How I treat NK/T-cell lymphomas. *Blood* 2013;121:4997–5005.
- de Mel S, Hue SS-S, Jeyasekharan AD, Chng W-J, Ng S-B. Molecular pathogenic pathways in extranodal NK/T cell lymphoma. *J Hematol Oncol* 2019;12:33.
- Somasundaram N, Lim JQ, Ong CK, Lim ST. Pathogenesis and biomarkers of natural killer T cell lymphoma (NKT). *J Hematol Oncol* 2019;12:28.
- Xiong J, Zhao W-L. Advances in multiple omics of natural-killer/T cell lymphoma. *J Hematol Oncol* 2018;11:134.
- Xiong J, Cui B-W, Wang N, Dai Y-T, Zhang H, Wang C-F. Genomic and transcriptomic characterization of natural killer T Cell lymphoma. *Cancer Cell* 2020;37:403–19 e6.
- Xu P-P, Xiong J, Cheng S, Zhao X, Wang C-F, Cai G. A phase II study of methotrexate, etoposide, dexamethasone and pegaspargase sandwiched with radiotherapy in the treatment of newly diagnosed, Stage IE to IIE extranodal natural-killer/T-cell lymphoma. Nasal-Type. *EBioMedicine*. 2017;25:41–9.
- Yamaguchi M, Suzuki R, Oguchi M. Advances in the treatment of extranodal NK/T-cell lymphoma, nasal type. *Blood* 2018;131:2528–40.
- Liu W-J, Wang H, Peng X-W, Wang W, Liu N-W, Wang Y. Asparagine synthetase expression is associated with the sensitivity to asparaginase in extranodal natural killer/T-cell lymphoma in vivo and in vitro. *Oncotargets Ther* 2018;11:6605–15.
- Di Meo A, Bartlett J, Cheng Y, Pasic MD, Yousef GM. Liquid biopsy: a step forward towards precision medicine in urologic malignancies. *Mol Cancer* 2017;16:80.
- Xiong J, Bian J, Wang L, Zhou J-Y, Wang Y, Zhao Y. Dysregulated choline metabolism in T-cell lymphoma: role of choline kinase- α and therapeutic targeting. *Blood Cancer J* 2015;5:287.
- Xiong J, Wang L, Fei X-C, Jiang X-F, Zheng Z, Zhao Y. MYC is a positive regulator of choline metabolism and impedes mitophagy-dependent necroptosis in diffuse large B-cell lymphoma. *Blood Cancer J* 2017;7:e0.
- Alexander SPH, Kelly E, Mathie A, Peters JA, Veale EL, Armstrong JF. THE CONCISE GUIDE TO PHARMACOLOGY 2019/20: transporters. *Br J Pharmacol* 2019;176:S397–493 Suppl 1.
- Kandasamy P, Gyimesi G, Kanai Y, Hediger MA. Amino acid transporters revisited: New views in health and disease. *Trends Biochem Sci* 2018;43:752–89.
- Chen W-L, Wang Y-Y, Zhao A, Xia L, Xie G, Su M. Enhanced fructose utilization mediated by SLC2A5 is a unique metabolic feature of acute myeloid leukemia with therapeutic potential. *Cancer Cell* 2016;30:779–91.
- Zhao P, Huang J, Zhang D, Zhang D, Wang F, Qu Y. SLC2A5 overexpression in childhood philadelphia chromosome-positive acute lymphoblastic leukaemia. *Br J Haematol* 2018;183:242–50.
- Grzes KM, Swamy M, Hukelmann JL, Emslie E, Sinclair LV, Cantrell DA. Control of amino acid transport coordinates metabolic reprogramming in T-cell malignancy. *Leukemia* 2017;31:2771–9.
- Qiu R, Shi H, Wang S, Leng S, Liu R, Zheng Y. BRMS1 coordinates with LSD1 and suppresses breast cancer cell metastasis. *Am J Cancer Res* 2018;8:2030–45.
- Fan H, Lu S, Wang S, Zhang S. Identification of critical genes associated with human osteosarcoma metastasis based on integrated gene expression profiling. *Mol Med Rep* 2019;20:915–30.
- Swerdlow SH, Campo E, Pileri SA, Harris NL, Stein H, Siebert R. The 2016 revision of the World Health Organization classification of lymphoid neoplasms. *Blood* 2016;127:2375–90.
- Kim D, Langmead B, Salzberg SL. HISAT: a fast spliced aligner with low memory requirements. *Nat Methods* 2015;12:357–60.
- Dobin A, Davis CA, Schlesinger F, Drenkow J, Zaleski C, Jha S. STAR: ultrafast universal RNA-seq aligner. *Bioinformatics* 2013;29:15–21.
- Shi W-Y, Xiao D, Wang L, Dong L-H, Yan Z-X, Shen Z-X. Therapeutic metformin/AMPK activation blocked lymphoma cell growth via inhibition of mTOR pathway and induction of autophagy. *Cell Death Dis* 2012;3:e275-e275.
- Smith CA, Want EJ, O'Maille G, Abagyan R, Siuzdak G. XCMS: processing mass spectrometry data for metabolite profiling using nonlinear peak alignment, matching, and identification. *Anal Chem* 2006;78:779–87.
- Zheng Z, Sun R, Zhao H-J, Fu D, Zhong H-J, Weng X-Q. MiR155 sensitized B-lymphoma cells to anti-PD-L1 antibody via PD-1/PD-L1-mediated lymphoma cell interaction with CD8+T cells. *Mol Cancer* 2019;18:54.
- Friedman J, Hastie T, Tibshirani R. Regularization paths for generalized linear models via coordinate descent. *J Statist Software* 2010;33:1–22.
- Bailey CG, Ryan RM, Thoeng AD, Ng C, King K, Vanslambrouck JM. Loss-of-function mutations in the glutamate transporter SLC1A1 cause human dicarboxylic aminoaciduria. *J Clin Invest* 2011;121:446–53.
- Altman BJ, Stine ZE, Dang CV. From Krebs to clinic: glutamine metabolism to cancer therapy. *Nat Rev Cancer* 2016;16:619–34.
- Drexler H, Matsuo Y. Malignant hematopoietic cell lines: in vitro models for the study of natural killer cell leukemia-lymphoma, 6.
- Nagato T, Kobayashi H, Kishibe K, Takahara M, Ogino T, Ishii H. Expression of interleukin-9 in nasal natural killer/T-Cell lymphoma cell lines and patients. *Clin Cancer Res* 2005;11:8250–7.
- Song TL, Nairismägi M-L, Laurensia Y, Lim J-Q, Tan J, Li Z-M. Oncogenic activation of the STAT3 pathway drives PD-L1 expression in natural killer/T-cell lymphoma. *Blood* 2018;132:1146–58.
- Momcilovic M, Bailey ST, Lee JT, Fishbein MC, Braas D, Go J. The GSK3 signaling axis regulates adaptive glutamine metabolism in lung squamous cell carcinoma. *Cancer Cell* 2018;33:905–921.e5.
- Pavlova NN, Hui S, Ghergurovich JM, Fan J, Intlekofer AM, White RM. As extracellular glutamine levels decline, asparagine becomes an essential amino acid. *Cell Metabolism* 2018;27:428–38 e5.
- Ma G, Liang Y, Chen Y, Wang L, Li D, Liang Z. Glutamine deprivation induces PD-L1 expression via activation of EGFR/ERK/c-Jun signaling in renal cancer. *Mol Cancer Res* 2020;18:324–39.
- Bian Y, Li W, Kremer DM, Sajjakulnukit P, Li S, Crespo J. Cancer SLC43A2 alters T cell methionine metabolism and histone methylation. *Nature* 2020;585:277–82.
- Villarino AV, Kanno Y, O'Shea JJ. Mechanisms and consequences of Jak-STAT signaling in the immune system. *Nat Immunol* 2017;18:374–84.
- Kim SJ, Yoon DH, Jaccard A, Chng WJ, Lim ST, Hong H. A prognostic index for natural killer cell lymphoma after non-anthracycline-based treatment: a multicentre, retrospective analysis. *Lancet Oncol* 2016;17:389–400.
- Li M, Chiang Y-L, Lyssiotis CA, Teater MR, Hong JY, Shen H. Non-oncogene addiction to SIRT3 plays a critical role in lymphomagenesis. *Cancer Cell* 2019;35:916–31 e9.
- Zhang L, Yao Y, Zhang S, Liu Y, Guo H, Ahmed M. Metabolic reprogramming toward oxidative phosphorylation identifies a therapeutic target for mantle cell lymphoma. *Sci Transl Med* 2019;11:eaau1167.
- Bröer A, Rahimi F, Bröer S. Deletion of Amino Acid Transporter ASCT2 (SLC1A5) Reveals an Essential Role for Transporters SNAT1 (SLC38A1) and SNAT2

- (SLC38A2) to Sustain Glutaminolysis in Cancer Cells. *J Biol Chem* 2016;291:13194–205.
- [40] Grewer C, Balani P, Weidenfeller C, Bartusel T, Tao Z, Rauen T. Individual subunits of the glutamate transporter EAAC1 homotrimer function independently of each other. *Biochemistry* 2005;44:11913–23.
- [41] Li Y, Shao H, Da Z, Pan J, Fu B. High expression of SLC38A1 predicts poor prognosis in patients with de novo acute myeloid leukemia. *J Cell Physiol* 2019;234:20322–8.
- [42] Pavlova NN, Hui S, Ghergurovich JM, Fan J, Intlekofer AM, White RM. As extracellular glutamine levels decline, asparagine becomes an essential amino acid. *Cell Metab* 2018;27:428–38 e5.
- [43] Leone RD, Powell JD. Metabolism of immune cells in cancer. *Nat Rev Cancer* 2020;20:516–31.
- [44] Leone RD, Zhao L, Englert JM, Sun I-M, Oh M-H, Sun I-H. Glutamine blockade induces divergent metabolic programs to overcome tumor immune evasion. *Science* 2019;366:1013–21.
- [45] Prestipino A, Emhardt AJ, Aumann K, O'Sullivan D, Gorantla SP, Duquesne S. Oncogenic JAK2V617F causes PD-L1 expression, mediating immune escape in myeloproliferative neoplasms. *Sci Transl Med* 2018;10.
- [46] Torrejon DY, Abril-Rodriguez G, Champhekar AS, Tsoi J, Campbell KM, Kalbasi A. Overcoming genetically based resistance mechanisms to PD-1 blockade. *Cancer Discov* 2020;10:1140–57.
- [47] Byun J-K, Park M, Lee S, Yun JW, Lee J, Kim JS. Inhibition of glutamine utilization synergizes with immune checkpoint inhibitor to promote antitumor immunity. *Molecular Cell* 2020;80:592–606 e8.